Influence of water transport and pore structure on the durability of porous building stones

D. BENAVENTE[1], J. MARTÍNEZ-MARTÍNEZ[2], G. ALGOZZINI[3] & M.A. GARCÍA DEL CURA[4]

[1] LPA. Dpto. CC Tierra y MA. Universidad de Alicante. (e-mail: david.benavente@ua.es)
[2] LPA. Dpto. CC Tierra y MA. Universidad de Alicante. (e-mail: javier.martinez@ua.es)
[3] LPA. Dpto. CC Tierra y MA. Universidad de Alicante.
[4] CSIC. LPA Unidad Asociada CSIC-UA.. (e-mail: angegcura@ua.es)

Abstract: The influence of both pore structure and water transport on the durability of porous building stones is evaluated. The aim of this study on porous building stones was to establish direct relationships between pore structure and water transport using a principal component analysis. The pore structure was described in terms of its porosity, pore size distribution (quantified by mean pore radius) and specific surface area whilst water transport was characterised by means of water permeability (saturated flow) and capillary imbibition (unsaturated flow).

The principal component analysis shows that there is a positive correlation between water transport coefficients (permeability and capillary absorption) and pore radius, whereas a negative correlation is recorded as regards surface area. A linear relationship between the square root of permeability and capillary absorption coefficient is also found, which may be easily estimated by means of a simple capillary imbibition test. Moreover, the principal component analysis presents the influences of water transport and pore structure parameters on durability, quantified by the percentage of weight loss after salt crystallization. Thus, durability has a negative correlation with pore radius and water transport coefficients, and a positive correlation with the surface area. As a consequence, water transport is closely related to pore structure properties and is a reliable indication of the durability of porous building stones.

Résumé: L'influence de la structure de pore et de l'écoulement de l'eau sur la longévité des pierres de construction poreuses est mesurée. L'objectif de cette étude sur les pierres de construction poreuses était d'établir les rapports directs entre la structure de pore et l'écoulement de l'eau grâce à l'analyse du constituant principal. La structure de pore a été mesurée en termes de porosité, de répartition de la taille de pore (mesuré en rayon moyen de pore) et de surface spécifique; et l'écoulement de l'eau est caractérisé par la moyenne de perméabilité à l'eau (flux saturé) et l'absorption capillaire (flux insaturé).

L'analyse du constituant principal montre qu'il existe une corrélation positive entre les coefficients d'écoulement de l'eau (perméabilité et absorption capillaire) et le rayon de pore, alors qu'il existe une corrélation négative avec la superficie. Il est aussi démontré une relation linéaire entre la racine carrée de la perméabilité et le coefficient d'absorption capillaire ; celle-ci peut être facilement utilisée pour mesurer d'après un simple test d'absorption capillaire. De plus, l'analyse du principal constituant montre l'influence des paramètres écoulement de l'eau et structure de pore sur la longévité, mesurée en pourcentage de masse perdue après cristallisation du sel. Ainsi, la longévité a une corrélation négative avec le rayon de pore et les coefficients d'écoulement de l'eau, et une corrélation positive avec la surface. Par conséquent, l'écoulement de l'eau est étroitement lié aux propriétés de structure de pore et est une information fiable sur la longévité des pierres de construction poreuses.

Keywords: Durability, Laboratory tests, Permeability, Porosity, Sedimentary rocks, Weathering.

INTRODUCTION

The durability of porous building rocks may be reduced when subjected to deterioration processes. In particular, salt crystallization is one of the most powerful weathering agents, especially when combined with frost activity (Jefferson, 1993). In porous materials, crystallisation pressure which depends on pore structure, the saturation degree of salt and the energy difference between the crystal and the pore wall is the most important decay mechanism that occurs during salt weathering (Scherer, 1999; Flatt, 2002). Most damage to porous building rocks is closely related to the dynamics of water movement, which depends on pore structure and controls the rate of supply solution and where precipitation occurs (Snethlage and Wendler, 1997; Rodriguez-Navarro and Doehne, 1999; Scherer, 2004). The presence of water in the rock enhances not only salt crystallization but also biodeterioration, material dissolution, the cyclic action of drying-wetting and freeze-thaw processes (Winkler, 1997; Camuffo, 1998). In this paper, we will examine direct relationships between durability during salt crystallisation processes and both pore structure and water transport properties, which are particularly interesting parameters for interpreting damage processes.

EXPERIMENTAL PROCEDURES

Materials

Several porous rocks, which are commonly used as building materials and/or belong to Architectural Heritage, have been chosen for this study due to their different petrophysical and petrological characteristics (Benavente, 2003). These stones are divided into two types of limestone, according to the Folk classification (1962): biocalcirudite (BR) and biocalcarenite (BC); and a siliceous stone or quartz-arenite (QA).

Biocalcirudites (and/or sandy biocalcirudites) (BR) are unsorted detrital stones with fragments of bryozoans, red algae, molluscs and echinoderm from 0.2 to 10 mm. The terrigenous fraction is comprised of quartz, limeclasts and feldspars. These biocalcirudites have abundant interparticle porosity, whereas intraparticle porosity is variable. Cement is scarce and consists mainly of microcrystalline drusy calcite.

Biocalcarenites (BC) or sandy fossiliferous limestones are well-sorted arenites. These stones contain foraminifers (mainly Globigerinae) ranging in size from 0.2 to 0.5 mm. Foraminifera shells are generally filled by glauconite and/or siliceous cement. The terrigenous fraction is comprised of quartz, feldspars, micas, dolostones and other rock fragments. Both interparticle and intraparticle porosity are variable. The most abundant type of cement present on these stones is equant-equicrystalline mosaics of calcite spar.

Quartzarenite (QA) is a well-sorted sandstone that consists of monocrystalline quartz grains with rare feldspars, metamorphic clasts, chert and muscovite grains. Primary interparticle porosity has been partially filled by silica crystallisation, which forms frequent overgrowths on quartz grains.

Porous Media Characterisation

Pore structure was described in terms of porosity, pore size distribution (quantified by the mean pore size, r_M,) and specific surface area (SSA), whilst characterisation was carried out using mercury intrusion porosimetry, the nitrogen absorption technique and the helium pyknometer.

Mercury porosimetry is extensively used for the characterisation of porous media. The connected porosity, P(Hg) and mean pore size, r_M, were obtained by Autopore IV 9500 Micromeritics mercury porosimetry (Table 1). The pore size interval ranges from 0.003 to 200 μm.

The determination of the specific surface area (SSA) of the samples was accomplished by using the nitrogen absorption technique. The determination of the SSA was carried out through the BET method (Rouquerol et al., 1994) and the points in the relative pressure interval $P/P_0 = 0.1 – 0.35$ were analysed by using the ASAP 2010 Micromeritics apparatus (Table 1).

The dry bulk density, ρ_{bulk}, of a rock is defined as the ratio of its mass to its volume, including the volume of voids and grains. In the characterisation test, 3 dried samples were used in the form of 30 mm diameter x 60 mm height cylinders (Table 1).

The true density, ρ_{true}, of a material is defined as the ratio of its mass to solid volume and can be obtained by using the Helium pyknometer. The real density was obtained by means of an AccuPyc 1330 device. The total porosity, P_T, was calculated using the following equation (Tiab and Donaldson, 1996):

$$P_T[\%] = \left(1 - \frac{\rho_{bulk}}{\rho_{true}}\right) \cdot 100 \quad (1)$$

Water Transport Characterisation

Water transport was characterized by means of liquid water permeability (saturated flow) and capillary imbibition (unsaturated flow). The capillary imbibition test is carried out using a continuous data-recorder. It allows automatic monitoring of the water uptake by the sample when its lower surface is in contact with the water reservoir. A schematic diagram of the experimental set-up is shown in Figure 1. The quasi-isolated chamber consists of a gastight methecrylate rectangle (40 x 40 x 60 cm^3) wherein stable moisture and temperature are achieved. An environmental sensor (HOBO® H8-Pro) is also placed in the chamber in order to control the stability of the environmental conditions. The balance device is linked to a computer, which automatically records weight gain in the tested specimen at specified intervals (every 10 seconds in the current study) using the code CK®.

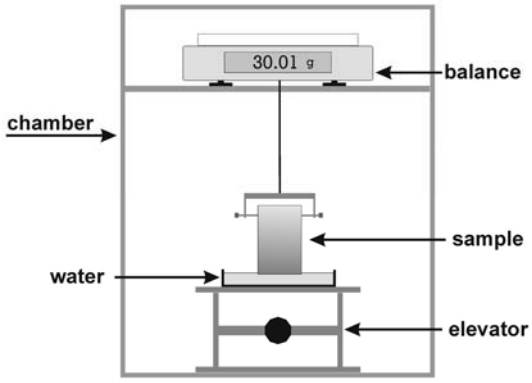

Figure 1. Schematic diagram of the set-up of the experiment for continuous capillary imbibition characterisation.

Three cylinder samples measuring 30 mm in diameter x 60 mm in height were used in each test. The sample was hung from the balance and the water container (20 x 30 x 5 cm^3) was raised with an elevator until water covers ~1mm of the sample height. This level was maintained constant during the test.

The temperature and relative humidity were constant throughout the experiment at 20 ± 1 ºC and 98 ± 0.5 % respectively. The results were plotted as absorbed water per area of the sample throughout imbibition versus the square root of time. Through this kind of representation, the capillary imbibition kinetic shows two parts. The first part defines capillary absorption and the second part defines saturation. The slope of the curve during capillary absorption is the capillary absorption coefficient, C.

The water permeability measurements were carried out in a triaxial cell (Figure 2). Water permeability (intrinsic permeability) was determined according to Darcy's Equation (Eq. (2)) when the steady-state flow was attained (water flow rate at inflow equals to water outflow rate):

$$k = \frac{\eta Q L}{A \Delta P} \tag{2}$$

where k is the coefficient of water permeability [mD] (1 D = $9.869 \cdot 10^{-13}$ m^2), η n the water viscosity, Q is the volumetric flow-rate of water, L is the length of the sample, A is the cross-sectional area of the sample perpendicular to the direction of flow and ΔP is the pressure gradient (Bear, 1998).

Pressure and volume changes were regulated by a pressure/volume controller, with accuracy below 1% in the pressure measurement and 0.5% over 100 cm^3 in the volume changes. The volumetric capacity is 250 cm^3. The volume changes and the confining and differential pressures are defined and controlled by using the code Mecasoft ®, which displayed on a X-Y plotter the flow rate versus time. A laminar (steady-state) flow rate with a constant pressure is achieved when the X-Y plot is a straight line. With this equipment, the permeability measurements are accurate for values below 500 mD (~$5 \cdot 10^{-13}$ m^2 or ~$5 \cdot 10^{-6}$ m/s for pure water at 20 ºC).

Permeability measurements were carried out with the same samples that were used in the dry density characterisation and in the capillary imbibition test. Thus, three cylinder samples measuring 30 mm in diameter x 60 mm in height were used after water saturation.

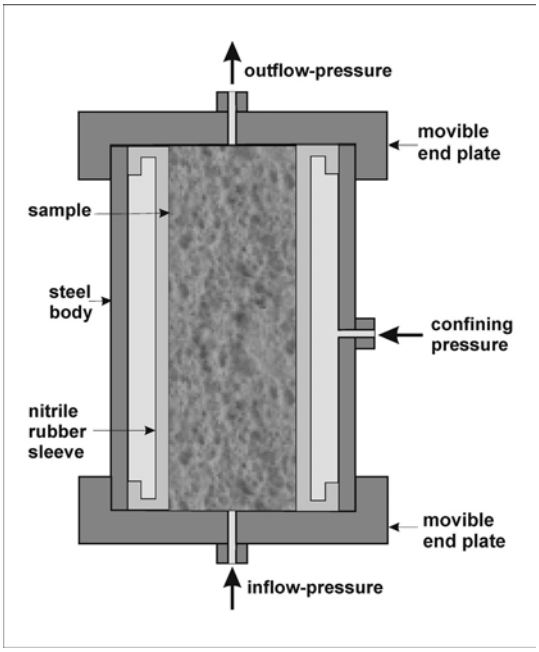

Figure 2. Schematic of triaxial cell for the water permeability measurements.

Salt Crystallisation Test

The salt crystallization test was performed using the continuous partial immersion test described by Benavente et al. (2001). Three samples were used in the form of 25×25×40 mm prisms and a 14 % w/w Na_2SO_4 solution was used. Resistance to salt crystallisation was found by performing the continuous partial immersion test, with 15 two-stage wetting-drying cycles, where the two stages were the capillary (40 ºC and 80% RH) and the precipitation stages (10 ºC and 70% RH). This is the procedure that most closely simulates the deterioration taking place in a construction material exposed to salt crystallisation. The samples were cleaned and dried (60 ºC) until they reached a constant weight. The dry weight loss (DWL) was calculated at this stage (Table 1).

Table 1. Connected porosity, P(Hg), and mean pore radius, r_M, obtained by mercury intrusion porosimetry; specific surface area, SSA; bulk, ρ_{bulk}, and true, ρ_{true}, density; total porosity P_T; capillary absorption coefficient, C; water permeability, k; and percentage of dry weight loss by salt crystallisation test, DWL, of the stones.

Sample	**P (Hg) [%]**	**r_M [μm]**	**SSA [m^2/g]**	**ρ_{bulk} [g/cm^3]**	**ρ_{true} [g/cm^3]**	**P_T [%]**	**C [$kg/(m^2 \cdot h^{0.5})$]**	**K [mD]**	**DWL [%]**
BR1	17.79	28.69	0.83	2.11	2.70	21.84	6.47	> 500	1.0
BR2	16.32	34.18	0.38	2.12	2.66	20.19	10.94	> 500	1.5
BC1	14.31	0.08	10.22	2.26	2.70	16.25	0.86	0.18	13.8
BC2	15.65	0.33	9.85	2.17	2.72	20.05	1.25	1.44	3.2
BC3	18.83	1.48	8.42	2.11	2.72	22.26	2.48	27.34	7.2
BC4	14.18	0.15	12.25	2.26	2.72	16.80	1.23	2.83	8.1
BC5	19.52	6.71	0.69	2.23	2.80	20.46	12.15	268.00	0.5
BC6	21.79	0.46	4.48	2.06	2.70	23.66	3.26	91.90	16.3
QA	13.48	2.43	2.31	2.28	2.67	14.62	1.68	13.34	0.5

RESULTS AND DISCUSSION

A principal component analysis (PCA) was performed in order to stabilise the structure of the variable dependence. This involved identifying relationships between variables and assigning a petrophysical meaning to each factor. The calculations were carried out with the SPSS® v.11.5.1 code. Two principal components were extracted which accounted for 83.8 % of the total variance, using Varimax as a factor rotation method (Figure 3).

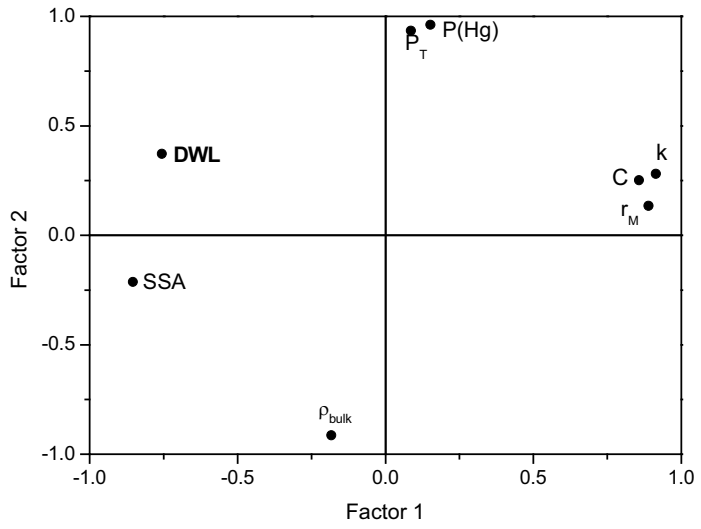

Figure 3. Principal component analysis considering connected porosity, P(Hg); mean pore radius, r_M; specific surface area, SSA; bulk density, ρ_{bulk}; total porosity P_T; capillary absorption coefficient, C; water permeability, k; and percentage of dry weight loss by salt crystallisation test, DWL.

The plot on the first component in Figure 3 shows that there is a positive correlation between water transport parameters (k and C) and mean pore radius, r_M, whereas a negative correlation with specific surface area, SSA is registered. The relationship between permeability and pore structure can be described from the Carmen-Kozeny equation, which expresses permeability as a function of pore size, r, and porosity, P (Bear, 1988; Dullien, 1992). Moreover, this equation can be expressed in terms of surface area per unit of grain volume, S_{Vgr}. The specific surface area per unit of grain volume, S_{Vgr} [m^{-1}], of a porous material is defined as the ratio of the surface area, A_S [m^2], exposed within the pore space to grain volume, V_{gr} [m^3] (Dullien, 1992; Tiab and Donaldson, 1996). Hence, specific surface area per unit of sample mass, SSA, is related to S_{Vgr} as follows:

$$S_{Vgr} = \frac{SSA}{\rho_{true}} . \tag{3}$$

Consequently, permeability is inversely proportional to the square of SSA, $k \propto 1/SSA^2$, and it reveals the inverse correlation between permeability and specific surface area obtained in the PCA.

The capillary flow is frequently interpreted by using the Washburn equation (1921)., which involves applying the Hagen-Poiseuille equation to the movement of the liquid meniscus in the porous solid. If the gravitational term is negligible, the net pressure driving force is the difference between the capillary pressure, ΔP, which can be written by the Laplace's equation as

$$\Delta P = \frac{2\gamma \cos\theta}{r}, \tag{4}$$

where γ is the interfacial tension and θ the contact angle. Therefore, the rise in the vertical direction, y, is described by the Washburn equation as:

$$y(t) = \sqrt{\frac{r^2 \cdot \Delta P}{4\eta} t} = \sqrt{\frac{r\gamma \cos\theta}{2\eta} t} = B\sqrt{t} . \tag{5}$$

The capillary absorption coefficient, C, obtained in the capillary imbibition test, is closely related to pore structure by pore radius and the porosity as follows (Mosquera et al., 2000; Benavente et al, 2002):

$$C = P\rho \sqrt{\frac{r\gamma \cos\theta}{2\eta}} , \tag{6}$$

where P is the porosity and ρ is the water density. Equation (6) explains the association of C and r_M observed in the PCA. This statistical analysis, moreover, indicate that there is a positive correlation between permeability, k, and capillary absorption coefficient, C. This association can be described by inserting the Carmen-Kozeny and Laplace's equations in Equation (6). Thus, the capillary absorption coefficient is related to the square root of the permeability, $C \propto \sqrt{k}$, taking into account that the rock is comprised of parallel capillary tubes (Zimmerman and Bodvarsson 1991). A linear relationship between the square root of the permeability and capillary absorption coefficient is described for rocks with k < 200 mD by:

$$\sqrt{k}\ [mD] = -3.01211 + 3.70 \cdot C[kg/m^2 \cdot s^{0.5}], \quad R = 0.9860. \tag{7}$$

Permeability measurements require more sophisticated equipment and experimental procedures than a capillary imbibition test. As a result, the permeability coefficient may be easily estimated for these kinds of porous materials from the capillary imbibition test, although further research into a wider range of rock types is needed in order to be able to fully apply the linear equation to estimate rock permeability.

The principal component analysis clearly shows the influence of water transport and pore structure parameters on the durability of porous building rocks under the effects of salt weathering. Durability, quantified by the percentage of weight loss after salt crystallization, DWL, has a negative correlation with the mean pore radius and water transport parameters (k and C), and a positive correlation with specific surface area, SSA.

Salt damage is closely related to pore size. According to Wellman and Wilson (1965), crystallisation occurs initially in the larger pores (forming large crystals, growing at the expense of the smaller) from solutions supplied by the smaller capillaries. The crystals will not grow in the smaller pores until high saturation is achieved (due to the large increase in the chemical potential of the crystal). Consequently, maximum crystallization pressure occurs when a large pore crystal grows in a pore with a small entrance.

When the pore liquid begins to evaporate, a meniscus develops in each pore, and the capillary pressure in the pore liquid decreases. As a result, capillary pressure induces flow between pores. If the evaporation rate is slower than capillary flow, then, evaporation occurs inside the rock, forming subfluorescence. In rocks with small pores, this phenomenon is particularly important (Scherer, 2004), and, moreover, it occurs far below the surface of the stone (Benavente et al, 2004b). Salt crystallization in porous stones mainly takes place on the surface of the porous stone (effluorescence), and within the porous media of stone (subfluorescence). Salt subfluorescence produces considerably more decay in porous stone than salt effluorescence. This is due to the fact that crystallization pressure on the stone is more effective when crystallization is produced within the stone mass (Winkler, 1997; Rodríguez-Navarro & Doehne 1999; Price 2000). Consequently, resistance to crystallization in porous rocks with small pores and low water transport coefficient values (C and k) tends to be reduced.

The specific surface area (SSA) of the materials is directly related to porosity and inversely related to pore size (Gregg and Sing, 1982). Materials with high porosity but small pore size (for example, BC1) presented a higher SSA than materials with a large pore radius and smaller porosity (for example, QA). From the PCA, the SSA appears to be directly related to durability (DWL values). Thus, high SSA values mean that a greater surface area of the material will be decayed. It is also inversely related to pore size, and, therefore, directly related to salt crystallization. Moreover, material with high SSA values implies a high capacity and susceptibility to water condensation and retention inside the materials. The presence of solutions favours not only salt weathering but also material dissolution, absorption of contamination gases, freeze-thaw action and biodeterioration.

On the other hand, a principal component analysis has also been carried out to stabilise associations between different kinds of rocks (Figure 4). A total of two factors justified 96.1 % of the total variance, using Varimax as a factor rotation method. The results indicate a clear separation of the samples mainly by water transport properties and pore size instead of durability characteristics. These rock associations represent rocks with low (BC1-BC2-BC4), medium (QA-BC3), and high (BC6-BC5-BR1-BR2) permeability values. The low influence of DWL in this classification may be interpreted by the influence of rock strength on salt weathering, which has not been included in this study. The susceptibility of porous rocks to the salt crystallization mechanism is closely connected to strength since it is the material's resistance to crystallization pressure (Benavente et al., 2004a).

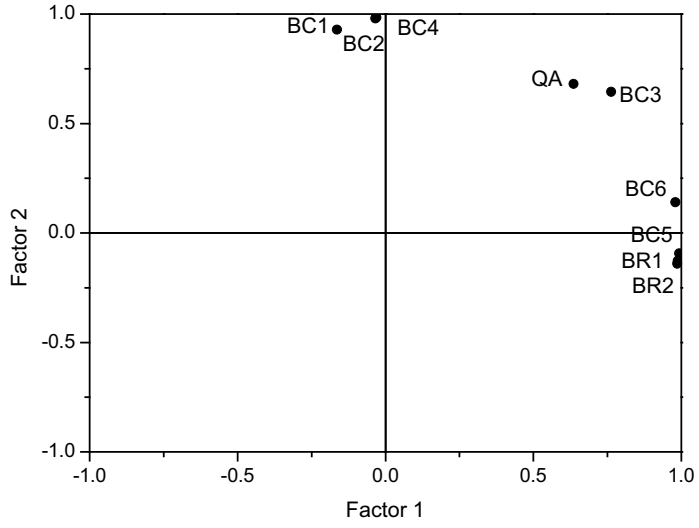

Figure 4. Principal component analysis applied to porous rocks: biocalcirudite, BR; biocalcarenite, BC, and quartz-arenite (QA).

CONCLUSIONS

In this study, the influence of both pore structure and water transport on porous building stone durability is approached using a principal component analysis.

The first component shows that there is a positive correlation between water transport parameters (k and C) and mean pore radius, whereas a negative correlation is registered with specific surface area. Moreover, this statistical analysis indicates that there is a positive correlation between permeability, k, and the capillary absorption coefficient, C. In particular, the capillary absorption coefficient is related to the square root of permeability, $C \propto \sqrt{k}$. This linear correction has a practical application since permeability measurements require more sophisticated equipment and experimental procedures than the capillary imbibition test.

Likewise, the principal component analysis shows the influences of water transport and pore structure parameters on the durability of porous building rocks affected by salt weathering processes. On the one hand, durability, quantified by the percentage of weight loss after salt crystallisation has a negative correlation with mean pore radius and water transport parameters (k and C). This correlation provides information about the role of solution transport in decay mechanisms, as regards solution supply and water evaporation rates. On the other hand, a positive correlation between durability and specific surface area, SSA, is also observed, which corroborates the inverse relationship of pore size with both SSA and salt crystallization pressure.

Finally, a principal component analysis has also been carried out in order to stabilise associations between different rocks. Results indicate a clear separation of the samples, mainly by water transport properties and pore size, instead of durability characteristics. This fact may be interpreted by the influence of rock strength on salt weathering, a factor that has not been included in this study.

Acknowledgements: This study was financed by the Generalitat Valenciana (Spain) through the Research Project GV05/129 and Research Group 03/158.

Corresponding author: Dr D. Benavente, Universidad de Alicante, Dpto. Ciencias de la Tierra y del Medio Ambiente, Alicante, 03080, Spain. Tel: +34 965903727. Email: david.benavente@ua.es.

REFERENCES

BEAR, J. 1988. *Dynamics of Fluids in Porous Media*. Elsevier, New York.

BENAVENTE, D. 2003. *Modelización y estimación de la durabilidad de materiales pétreos porosos frente a la cristalización de sales*. Biblioteca Virtual Miguel de Cervantes, <http://www.cervantesvirtual.com/FichaObra.html?Ref=12011> Accessed: 18/11/2005.

BENAVENTE, D., GARCÍA DEL CURA, M.A., BERNABÉU, A. & ORDÓÑEZ, S. 2001. Quantification of salt weathering in porous stones using an experimental continuous partial immersion method. *Engineering Geology*, **59**, 313-325.

BENAVENTE, D., GARCÍA DEL CURA M.A., FORT, R. & ORDÓÑEZ, S. 2004a. Durability estimation of porous building stones from pore structure and strength. *Engineering Geology*, **74**, 113-127.

BENAVENTE, D., GARCÍA DEL CURA, M.A., GARCIA-GUINEA, J., SANCHEZ-MORAL, S. & ORDÓÑEZ, S. 2004b. Role of pore structure in salt crystallisation in unsaturated porous stone. *Journal of Crystal Growth*, **260** (3-4): 532-544 JAN 9 2004

BENAVENTE, D., LOCK, P., GARCÍA DEL CURA, M.A., & ORDÓÑEZ, S. 2002. Predicting the capillary imbibition of porous rocks from microstructure. *Transport in Porous Media*, **49**, 59-76.

CAMUFFO, D. 1998. *Microclimate for Cultural Heritage*. Elsevier, Amsterdam.

DULLIEN, F.A.L. 1992. *Porous Media Fluid Transport and Pore Structure*. Academic Press. San Diego.

FLATT, R.J. 2002. Salt damage in porous materials: how high supersaturations are generated. *Journal of Crystal Growth*, **242**, 435-454.

FOLK, R. 1962. Spectral subdivision of limestone types. In: Ham, W.E. (ed.) Classification of Carbonate Rocks. *Memoirs of the American Association of Petroleum Geologists*, **1**, 62-84.

GREGG, S.J. & SING, K.S.W. 1982. *Adsorption, surface area, and porosity*. 2nd Edition, Academic Press, London.

JEFFERSON, D. P. 1993. Building stone: the geological dimension. *Quarterly Journal of Engineering Geology*, **26**, 305-319.

MOSQUERA, M.J., RIVAS, T., PRIETO, B. & SILVA, B. 2000. Capillary rise in granitic rocks: Interpretation of kinetics on the basis of pore structure. *Journal of Colloid and Interface Science*, **222**, 41-45.

PRICE, C.A. *An Expert Chemical Model for Determining the Environmental Conditions Needed to Prevent Damage in Porous Materials*. Archetype Publications Ltd., London, 2000.

RODRÍGUEZ-NAVARRO, C. & DOEHNE, E. 1999. Salt weathering: influence of evaporation rate, supersaturation and crystallisation pattern. *Earth Surface Processes and Landforms*, **24**, 191-209.

Rouquerol, J., Avnir, D., Fairbridge, C.W., Everett, D.H., Haynes, J.H., Pernicone, N., Ramsay, J.D.F., Sing, K.S.W. & Unger, K.K. 1994. Recommendations for the characterization of porous solids. *Pure and Applied Chemistry*, **66**, 1739-1758.

SCHERER, G.W. 1999. Crystallisation in pores. *Cement and Concrete Research*, **29**, 1347-1358.

SCHERER, G.W. 2004. Stress from crystallization of salt. *Cement and Concrete Research*, **34**, 1613-1624.

SNETHLAGE, R. & WENDLER, E. 1997. Moisture cycles and sandstone degradation. In *Saving Our Architecture Heritage: The Conservation Historic Stone Structures* (N.S. Baer y R. Snethlage ed.) John Wiley & Sons, Chichester, 7-24.

TIAB, D. & DONALDSON, E.C. 1996. *Petrophysics: theory and practice of measuring reservoir rock and fluid transport properties*. Gulf Publishing Company, Houston, Texas.

WASHBURN, E. W. 1921. The dynamics of capillary flow. *Physical Review*, **17**, 273-283.

WELLMAN, H.W. & WILSON, A.T. 1965. Salt weathering, a neglected geological erosive agent in coastal and arid environments. *Nature*, **205**, 1097-1098.

WINKLER, E.M. 1997. *Stone in Architecture: Properties, Durability*. 3rd Edition, Springer-Verlag, Berlin.
ZIMMERMAN, R. W. & BODVARSSON, G. 1991. A simple approximate solution for horizontal infiltration in a Brooks-Corey medium. *Transport in Porous Media*, **6**,195-205.